

This article was downloaded by: [University Of Gujrat]

On: 11 December 2014, At: 13:44

Publisher: Taylor & Francis

Informa Ltd Registered in England and Wales Registered Number: 1072954 Registered office: Mortimer House, 37-41 Mortimer Street, London W1T 3JH, UK



Molecular Crystals and Liquid Crystals

Publication details, including instructions for authors and subscription information:

<http://www.tandfonline.com/loi/gmcl20>

CdSe Quantum Dot-sensitized, Nanoporous p-type NiO Photocathodes for Quantum Dot-sensitized Solar Cells

Min-Ah Park^a, Soo-Yong Lee^a, Jae-Hong Kim^a, Soon-Hyung Kang^b, Hyunsoo Kim^c, Chel-Jong Choi^c & Kwang-Soon Ahn^a

^a School of Chemical Engineering, Yeungnam University, Gyeongsan, S. Korea

^b Department of Chemistry Education, Chonnam National University, Gwangju, S. Korea

^c School of Semiconductor and Chemical Engineering, Chonbuk National University, Jeonju, S. Korea

Published online: 17 Nov 2014.

To cite this article: Min-Ah Park, Soo-Yong Lee, Jae-Hong Kim, Soon-Hyung Kang, Hyunsoo Kim, Chel-Jong Choi & Kwang-Soon Ahn (2014) CdSe Quantum Dot-sensitized, Nanoporous p-type NiO Photocathodes for Quantum Dot-sensitized Solar Cells, *Molecular Crystals and Liquid Crystals*, 598:1, 154-162, DOI: [10.1080/15421406.2014.933387](http://dx.doi.org/10.1080/15421406.2014.933387)

To link to this article: <http://dx.doi.org/10.1080/15421406.2014.933387>

PLEASE SCROLL DOWN FOR ARTICLE

Taylor & Francis makes every effort to ensure the accuracy of all the information (the "Content") contained in the publications on our platform. However, Taylor & Francis, our agents, and our licensors make no representations or warranties whatsoever as to the accuracy, completeness, or suitability for any purpose of the Content. Any opinions and views expressed in this publication are the opinions and views of the authors, and are not the views of or endorsed by Taylor & Francis. The accuracy of the Content should not be relied upon and should be independently verified with primary sources of information. Taylor and Francis shall not be liable for any losses, actions, claims, proceedings, demands, costs, expenses, damages, and other liabilities whatsoever or howsoever caused arising directly or indirectly in connection with, in relation to or arising out of the use of the Content.

This article may be used for research, teaching, and private study purposes. Any substantial or systematic reproduction, redistribution, reselling, loan, sub-licensing, systematic supply, or distribution in any form to anyone is expressly forbidden. Terms &

CdSe Quantum Dot-sensitized, Nanoporous p-type NiO Photocathodes for Quantum Dot-sensitized Solar Cells

MIN-AH PARK,¹ SOO-YONG LEE,¹ JAE-HONG KIM,¹
SOON-HYUNG KANG,² HYUNSOO KIM,³
CHEL-JONG CHOI,^{3,*} AND KWANG-SOON AHN^{1,*}

¹School of Chemical Engineering, Yeungnam University, Gyeongsan, S. Korea

²Department of Chemistry Education, Chonnam National University,
Gwangju, S. Korea

³School of Semiconductor and Chemical Engineering, Chonbuk National
University, Jeonju, S. Korea

CdSe quantum dots (QDs) were deposited on a p-type nanoporous NiO surface by repeating the successive ionic layer adsorption and reaction (SILAR) procedure 6, 9, 12, and 15 times. The NiO/CdSe prepared using 12 SILAR cycles, which is denoted as the NiO/CdSe(12), exhibited a larger QD size and better QD coverage on the nanoporous NiO than the NiO films with CdSe(6) and CdSe(9), leading to better light absorption over longer wavelengths and a significantly increased hole lifetime. The resulting quantum dot-sensitized solar cell (QD-SSC) exhibited significantly enhanced cell efficiency (0.35%) compared to that (0.013%) of the QD-SSC with the NiO/CdSe(6). NiO/CdSe(15), however, exhibited a lower hole lifetime and hindered ion transport as a result of the agglomeration of QDs as well as the severely blocked pores of the nanoporous NiO, causing a significantly reduced cell efficiency for QD-SSCs with NiO/CdSe(15).

Keywords Quantum dot-sensitized solar cell; p-type NiO; hole lifetime; ion transport

1. Introduction

Semiconducting quantum dots (QDs), such as CdS, CdSe, PbS, and InP, have been tested as photo-sensitizers for the next generation solar cells [1–5] because their optical band gaps can be adjusted easily through the size dependent quantum confinement effects [1–5]. In addition, these materials are robust, inorganic materials with higher extinction coefficients due to the existence of multiple levels [1–5]. Quantum dot-sensitized solar cells (QD-SSCs) adopt the design of dye-sensitized solar cells (DSSCs). Most QD-SSCs are based on the sensitization of a nanoporous wide band gap n-type semiconductor. The

Both Prof. K.-S. Ahn and C.-J. Choi contributed equally to this work as the corresponding authors.

*Address correspondence to C.-J. Choi and K.-S. Ahn Tel.: +82-53-810-2524. Fax: +82-53-810-4631. E-mail: cjchoi@jbnu.ac.kr; kstheory@ynu.ac.kr

Color versions of one or more of the figures in the article can be found online at www.tandfonline.com/gmcl.

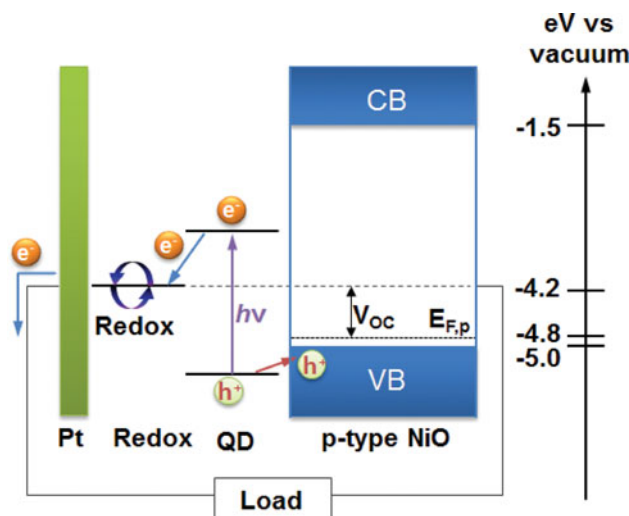


Figure 1. Energy-level diagram for the operation of QD-SSCs with a p-type NiO.

cell efficiency as high as 5% was reported in the n-type semiconducting TiO_2 -based photoanodes. The QD-sensitized photocathodes using the p-type semiconductors operate in the reverse mode, where the photocurrents result from the hole injection from the QDs into the p-type semiconductors. Combination of such p-type and n-type QD-SSCs allows to construct the tandem photoelectrochemical solar cells, which provide the higher cell voltages and theoretically higher cell performances than single-junction QD-SSCs [6–8]. However, the efficiencies of the tandem QD-SSCs are limited by the poor performance of the p-type QD-SSC. Only a limited number of studies of quantum dot-sensitized p-type semiconductors have been reported, and the energy conversion efficiency of the cells is quite low [9–11]. Therefore, the cell performances of the QD-SSCs with the p-type photocathodes have yet to be significantly improved for the realization of the highly efficient tandem QD-SSCs.

NiO is used most widely as a wide band gap p-type semiconductor for sensitized photocathodes because its good stability and transparency [6–12]. Figure 1 presents an energy-level diagram showing the operation of QD-SSCs with p-type NiO [9–11]. The valence band maximum and the conduction band minimum of the NiO are -5.0 and -1.5 eV, respectively [9]. Assuming that the position of the quasi-Fermi level of the holes in the NiO has approximately 0.2 V difference from that of the valence band [9], the quasi-Fermi level of the NiO is -4.8 eV. The polysulfide electrolyte has the redox potential of -4.2 eV. Unlike n-type semiconductor-based QD-SSCs, the QDs assembled on a NiO surface can be excited through light absorption. Electrons photoexcited in QDs are injected into the redox couple, whereas the holes are transferred through the valence band (VB) of NiO to the transparent conducting oxide (TCO).

Q. Wang's group [13] fabricated the NiO sensitized by the cascaded CdS/CdSe and compared this structure with the NiOs with the CdS only and CdSe only. In this article, CdSe QDs were deposited *in situ* on a p-type NiO surface by repeating the successive ionic layer adsorption and reaction (SILAR) procedure 6, 9, 12, to 15 times. The cell performances were studied with the different SILAR cycles of the CdSe, which was discussed in terms of the morphology, optical absorption, carrier lifetime, and recombination rate on the photosensitization of nanoporous p-type NiO using CdSe QDs. The QD-SSC fabricated

by the optimized CdSe QDs exhibited an overall energy conversion efficiency as high as 0.35% under 1 sun illumination.

2. Experimental

2.1. Preparation of Nanoporous p-type NiO Films

A NiO colloidal solution containing 15 g of NiO nanopowder (Inframat) and 45 mL of ethanol was dispersed with zirconia. A NiO paste was produced by mixing the NiO solution, ethyl cellulose (Tokyo kasei) and 100 mL terpineol (Kanto chemical), followed by evaporating the ethanol with a rotary evaporator at 80°C for 40 min. The ethyl cellulose concentration in ethanol was 10 wt%.

Nanoporous NiO films were prepared by doctor-blading a NiO paste on a fluorine-doped tin oxide (FTO)-coated glass substrate, followed by drying in an oven for 30 min and sintering at 450°C for 30 min. The films were deposited to a thickness of 6.5 μm , as measured by stylus profilometry, and the active area was approximately 0.2 cm^2 .

2.2. Preparation of CdSe QD-assembled NiO Films

CdSe QDs were assembled on NiO films by SILAR [4,14]. For the synthesis of CdSe QDs, ethanol was used to dissolve 30 mM $\text{Cd}(\text{NO}_3)_2$ and sodium selenide in a glove box, respectively. Sodium selenide was prepared from 30 mM SeO_2 and 60 mM NaBH_4 solutions. The SILAR process involved immersing the NiO films in a $\text{Cd}(\text{NO}_3)_2$ solution for 1 min, rinsing it with ethanol, followed by further immersion in a sodium selenide solution for 1 min, and rinsing with ethanol. Each two-step immersion constituted a single SILAR cycle. The SILAR procedure was carried out on NiO samples for 6, 9, 12, and 15 cycles, which are referred to as NiO/CdSe(cycle number) for simplicity.

2.3. Cell Fabrication and Characterization

Semitransparent Pt counter electrodes (CEs) were prepared by doctor-blading a Pt nanocluster-containing Pt paste (PT-1, Dyesol. Ltd.) onto FTO substrates followed by calcination at 450°C for 30 min in air. The CdSe QD-assembled NiO films and Pt counter electrodes were sandwiched using a 60 μm -thick sealing material. A polysulfide electrolyte containing 0.5 M Na_2S , 1 M S, and 0.2 M KCl was prepared using methanol as the solvent.

The QD-SSCs were illuminated from the front side, i.e. from the QD-assembled NiO photocathode. Their photovoltaic current-voltage characteristics were measured using a solar simulator (PEC-L11, Peccell Ltd.) under 1 sun illumination (100 mWcm^{-2} , AM 1.5) which was verified using an AIST-calibrated Si-solar cell. For the open-circuit voltage decay (OCVD) measurements, the cells were illuminated to a steady voltage and the decay in the open-circuit voltage was measured after illumination was blocked with a shutter. The CdSe QDs assembled on NiO were characterized by UV-Vis absorbance spectroscopy (Cary5000, Agilent Tech. Co.). The crystallographic structure and grain size of the NiO were characterized by X-ray diffraction (XRD, PANalytical) and the morphology of the CdSe QD-assembled NiO films was examined by scanning electron microscopy (SEM, Hitachi FE-SEM S4800).

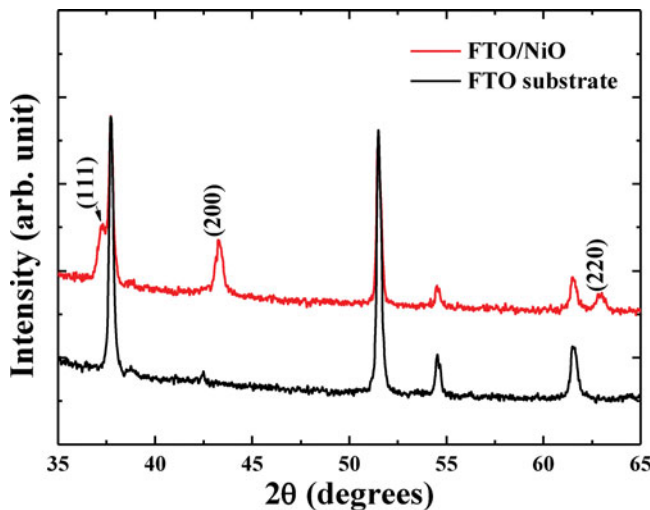


Figure 2. X-ray diffraction (XRD) patterns of the FTO substrate and NiO deposited on FTO.

3. Results and Discussion

Figure 2 shows the XRD patterns of the FTO substrate and NiO on the FTO. The NiO exhibited characteristic peaks of (111), (200) and (220), corresponding the face-centered cubic NiO phase (JCPDS 4-835). The mean grain size of the NiO was approximately 14.5 nm, as estimated by the Sherrer equation using the (200) peak.

Figure 3 shows FE-SEM images of the surface morphology of the bare nanoporous NiO film and NiO films sensitized by CdSe (6, 12 and 15). The bare NiO film exhibited highly porous nanostructures of NiO nanoparticles. As the number of SILAR cycles was increased, the CdSe QDs grew thicker on the NiO surface, increasing their size. The pore sizes in the films decreased with increasing number of SILAR cycles so that the NiO/CdSe(15) exhibited severely blocked pores. This is attributed to the excess growth and agglomeration of the CdSe QDs, which likely restricts the movement of the redox couple ions through the pores, hindering ion transport.

Figure 4 shows (a) the optical absorbance spectra of the bare nanoporous NiO and nanoporous NiO films sensitized by the CdSe QD (6, 9, 12, and 15). In this experiment, the QDs were assembled by the SILAR process. The SILAR has the advantages of *in situ* deposition and better coverage of the QDs on the surface, compared with the pre-synthesis method. However, it has the disadvantages of inhomogeneous distribution of the QDs, and so it was too difficult to evaluate the exact amount of the deposited QDs. The absorbance increased with increasing number of SILAR cycles, indicating a larger amount of CdSe QDs deposited. In addition, due to the size quantization effect, the absorbance shoulder and absorbance onset showed a red shift with increasing number of SILAR cycles, indicating the sequential growth of CdSe QDs. The mean diameter of the CdSe QDs was estimated using the Brus equation [3, 15]

$$E_{QD} = E_g + \frac{h^2}{8r^2} \left[\frac{1}{m_e^*} + \frac{1}{m_h^*} \right] - \frac{1.8e^2}{4\pi\epsilon\epsilon_0 r} \quad (1)$$

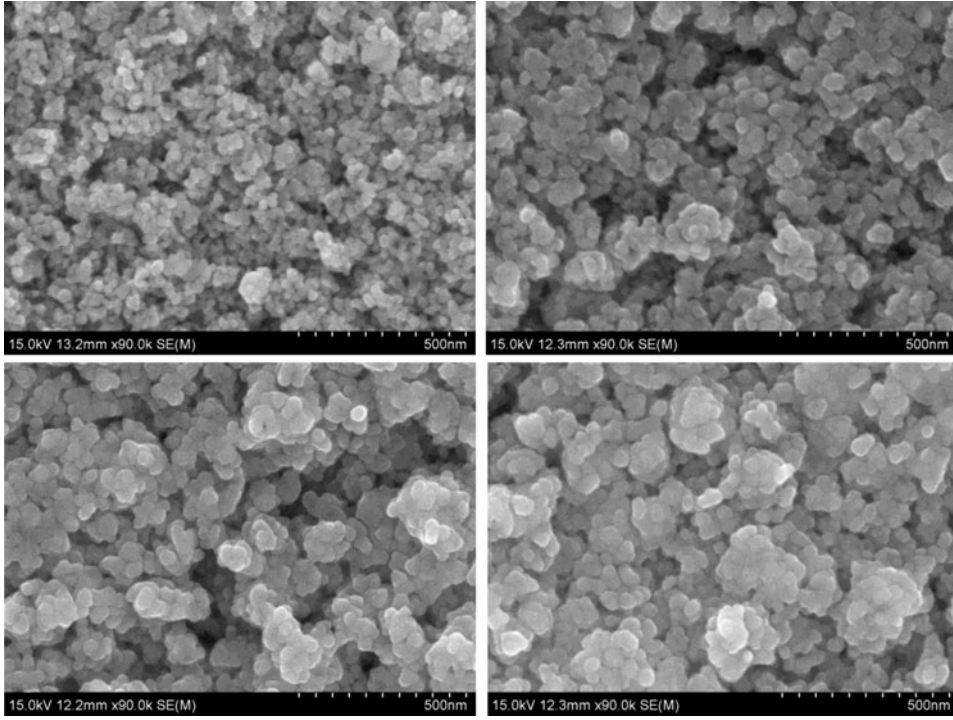


Figure 3. FE-SEM images of the (a) bare nanoporous NiO film and (b, c, d) the NiO films sensitized by CdSe(6), CdSe(12), and CdSe(15), respectively.

where E_{QD} and E_g are the lowest excitation energy of the QDs and the band gap (1.65 eV) of bulk CdSe particles, respectively, r is the radius of the QDs, m_e^* and m_h^* are the effective masses of electrons and holes, respectively, ϵ_0 is the vacuum permittivity, and ϵ is the relative permittivity. The optical band gaps of the QDs were estimated from the Tauc plots [Fig. 4(b)]. The mean size of the CdSe QDs was estimated to be 3.8, 4.2, 4.8, and 5.4 nm for the CdSe(6), CdSe(9), CdSe(12), and CdSe(13) assembled on the NiO films, respectively.

Figure 5 shows the open circuit voltage (V_{oc}) decay transients of the QD-SSCs recorded during relaxation from the illuminated quasi-equilibrium state to darkness. The carrier lifetimes are related to the V_{oc} decay transients according to the following equation [16, 17]:

$$\tau = - \frac{k_B T}{e} \left[\frac{dV_{oc}}{dt} \right]^{-1} \quad (2)$$

where $k_B T$ is the thermal energy, e is the positive elementary charge and dV_{oc}/dt is the derivative of the open circuit voltage transient. The V_{oc} is the potential difference between the quasi-Fermi level of the p-type NiO and the redox couple in the electrolyte, suggesting that the V_{oc} decay is related to the lower number of the holes in the valence band of NiO. That is, the hole lifetime depends strongly on back hole transfer from NiO to the redox couple and/or the CdSe. The hole lifetimes quantitatively estimated at 0.15 V using the equation (2) were listed in the Table 1. The V_{oc} decayed more slowly when the SLAR procedure was increased to 12 cycles, indicating the increased hole lifetime. This is because

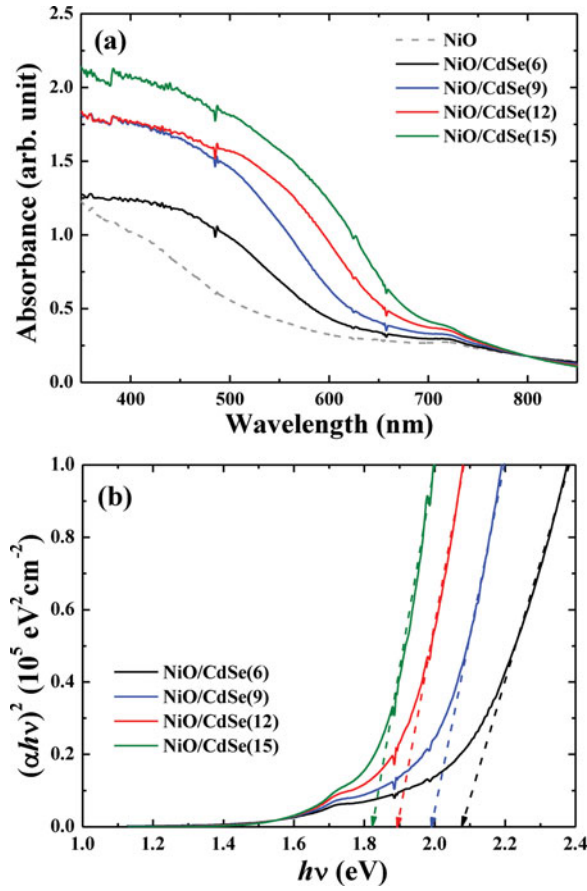


Figure 4. (a) Optical absorbance curves of the bare and CdSe QD-assembled NiO films. (b) Tauc plot of the CdSe-assembled NiO films.

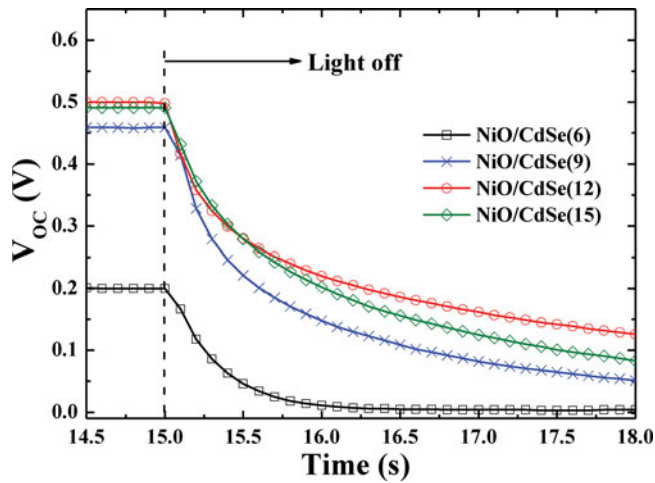


Figure 5. Open-circuit voltage decay curves of the NiO/CdSe(6, 9, 12, and 15) films.

Table 1. Photovoltaic performance of the QD-SSCs measured under 1 sun illumination

Samples	J_{sc} /mAcm ⁻²	V_{oc} /V	FF /%	η /%	Hole lifetime* /ms
NiO/CdSe(6)	0.22	0.19	31	0.013	32
NiO/CdSe(9)	0.89	0.46	28	0.12	122
NiO/CdSe(12)	3.04	0.49	23	0.35	329
NiO/CdSe(15)	1.70	0.46	21	0.16	226

*Calculated at 0.15 V using the equation (2)

the increased QD size and better coverage on the NiO surface at the larger number of CdSe SILAR cycles reduced the interfacial contact area between NiO and the electrolyte, leading to less back hole transfer from the NiO to the redox couple. In contrast, the V_{oc} of the NiO/CdSe(15) decayed more rapidly than that of the NiO/CdSe(12), indicating a reduced hole lifetime. This is because the agglomerated CdSe(15) QDs include many more defect states, facilitating trap-mediated recombination between the holes in the NiO and electrons in the CdSe. A detailed study in this area is currently underway.

Figure 6 shows the photovoltaic current-voltage performance of the QD-SSCs with p-type nanoporous NiO films sensitized by CdSe QD (6, 9, 12, and 15) measured under the 1 sun illumination, which is summarized in Table 1. These results were very reproducible. Overall, all the QD-SSCs exhibited poor fill factors due to the poor hole mobility of the nanoporous p-type NiO [11]. The QD-SSC with NiO/CdSe(12) exhibited the highest overall energy conversion efficiency of 0.35% compared to that with NiO/CdSe(6), due to the significantly improved short-circuit current and open-circuit voltage. This was attributed to the increased QD size and better coverage of CdSe(12), because these led to better light absorption over the longer wavelengths and the significantly increased hole lifetime. The V_{oc} is closely related to the charge injection and the recombination rate. The better light absorption and enhanced hole lifetime lead to the higher charge injection and the

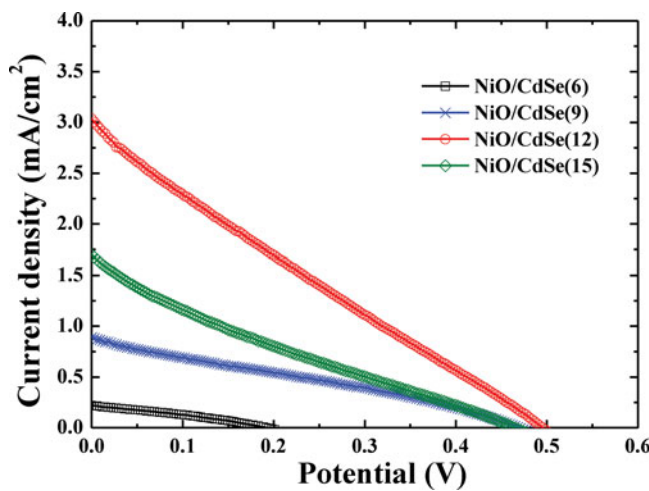


Figure 6. Photovoltaic current-voltage performance of the QD-SSCs with the NiO/CdSe(6, 9, 12, and 15) films measured under 1 sun illumination.

reduced recombination, which contributed to the highest V_{oc} value of the QD-SSC with the NiO/CdSe(12). On the other hand, although the NiO film sensitized by CdSe(15) exhibited the lowest optical band gap among the other samples, the cell efficiency with NiO/CdSe(15) was much lower than that with the NiO/CdSe(12) due to the significantly lower short-circuit current and the reduced V_{oc} . The agglomerated QDs and the blocked pores in the NiO/CdSe(15) film led to a facilitated recombination rate (or reduced hole lifetime) and hindered ion transport, respectively, which is responsible for the reduced J_{sc} and V_{oc} values.

4. Conclusions

The CdSe QDs were assembled *in situ* on the p-type nanoporous NiO surface by repeating the SILAR procedure (6, 9, 12, to 15 cycles). The QD-SSC with the NiO/CdSe(12) exhibited the best cell efficiency of 0.35% compared to the cell performance (0.013%) of the QD-SSC with the NiO/CdSe(6). This was attributed to the better light absorption over the long wavelengths and the significantly longer hole lifetime caused by the increased QDs size and better coverage of the CdSe(12). On the other hand, the QD-SSCs with the NiO/CdSe(15) exhibited lower cell efficiency (0.16%) compared to that with NiO/CdSe(12) due to the reduced hole lifetime and hindered ion transport caused by the agglomerated QDs and the blocked pores in NiO/CdSe(15), respectively. These results highlight the potential of quantum dots on p-type oxides for a range of applications, such as solar cells, catalysts and photoelectrochemical cells.

Acknowledgments

This study was supported by Basic Science Research Program through the National Research Foundation of Korea (NRF) funded by the Ministry of Education, Science and Technology (grant number 2012R1A1A4A01009654) and also by the Human Resources Development Program of Korea Institute of Energy Technology Evaluation and Planning (KETEP) grant (No. 20104010100580) funded by the Korean Ministry of Knowledge Economy.

References

- [1] Hodes, G. (2008). *J. Phys. Chem. C*, 112, 17778.
- [2] Chang, C.-H., & Lee, Y.-L. (2007). *Appl. Phys. Lett.*, 91, 053503.
- [3] Lee, W. J., Kang, S.-H., Min, S. K., Sung, Y.-E., & Han, S.-H. (2008). *Electrochem. Commun.*, 10, 1579.
- [4] Kim, H. S., Jung, S.-W., Ahn, K.-S., & Kang, S. H. (2013). *Current Appl. Phys.*, 13, S162.
- [5] Yang, Z., Chen, C.-Y., Roy, P., & Chang, H.-T. (2011). *Chem. Commun.*, 47, 9561.
- [6] He, J., Lindström, H., Hagfeldt, A., & Lindquist, S.-E. (2000). *Sol. Energy Mater. & Solar cells*, 6, 265.
- [7] Nattestad, A., Mozer, A. J., Fischer, M. K. R., Cheng, Y.-B., Mishra, A., Bäuerle, P., & Bach, U. (2010). *Nature Mater.*, 9, 31.
- [8] He, J., Lindström, H., Hagfeldt, A., & Lindquist, S.-E. (1999). *J. Phys. Chem. B*, 103, 8940.
- [9] Kang, S.-H., Zhu, K., Neale, N. R., & Frank, A. J. (2011). *Chem. Commun.*, 47, 10419.
- [10] Rhee, J. H., Lee, Y. H., Bera, P., & Seok, S. I. (2009). *Chem. Phys. Lett.*, 477, 345.
- [11] Chan, X.-H., Jennings, J. R., Hossain, M. A., Yu, K. K. Z., & Wang, Q. (2011). *J. Electrochem. Soc.*, 158, H733.
- [12] Mishra, A., Fischer, M. K. R., & Bäuerle, P. (2009). *Angew. Chem. Int. Ed.*, 48, 2474.

- [13] Safari-Alamuti, F., Jennings, J. R., Hossain, M. A., Yung, L. Y. L., & Wang, Q. (2013). *Phys. Chem. Chem. Phys.*, 15, 4767.
- [14] Lee, H.-J., Wang, M., Chen, P., Gamelin, D. R., Zakeeruddin S. M., Grätzel, M., & Nazeeruddin, M. K. (2009). *Nano Lett.*, 9, 4221.
- [15] Huang, S., Zhang, Q., Huang, X., Guo, X., Deng, M., Li, D., Luo, Y., Shen, Q., Toyoda, T., Meng, Q. (2010). *Nanotechnol.*, 21, 3752021.
- [16] Zaban, A., Greenshtein, M., & Bisquert, J. (2003). *Chem. Phys. Chem*, 4, 859.
- [17] Liu, Z., Miyauchi, M., Uemura, Y., Cui, Y., Hara, K., Zhao, Z., Sunahara, K., & Furube, A. (2010). *Appl. Phys. Lett.*, 96, 233107.